Computational Mechanics 29 (2002) 61–67 © Springer-Verlag 2002
DOI 10.1007/s00466-002-0324-0

Modeling and simulation of progressive penetration of multilayered ballistic fabric shielding

T. I. Zohdi

Abstract In this paper a simulation technique is developed to estimate the number of ballistic fabric sheets needed to stop an incoming projectile. Such sheets are free of any fortification by a resin. The computational approach is designed so that it can be easily implemented by a wide audience of researchers in the field, without resorting to more involved finite element formulations. This is achieved by taking advantage of the intrinsic characteristics of such fabric structures. Since the deformations of the fabric are (a) finite, (b) nonlinearly inelastic due to progressive fiber degradation and (c) dynamically coupled to the projectile, the system is highly nonlinear. A temporally adaptive, iterative scheme is developed to solve the system. Theoretical issues pertaining to convergence of the algorithm are investigated. Large-scale 3-D numerical examples are then given to illustrate the approach in determining the number of sheets needed to stop a projectile.

Keywords Ballistic fabric shielding, Large-scale simulation

1 Introduction

During the past three decades, lightweight ballistic fabric has owed its success largely to the incorporation of high strength polymeric fibers. Applications range from body armor to the protection of mission-critical military and commercial structural components. For overviews, recent applications, models, and case studies see Roylance and Wang [20], Taylor and Vinson [25], Shim et al. [21], Shockey et al. [22], Johnson et al. [11], Tabiei and Jiang [24] Kollegal and Sridharan [13], Simons et al. [23] and Walker [27]. A primary current concern is to determine the number of sheets of ballistic fabric shielding needed to stop an incoming projectile. Such sheets are free of any fortification by a solid resin. Experimental ballistic tests on such materials are extremely expensive and time consuming. Therefore, it is advantageous to employ computational simulations to reduce the number of tests needed for evaluations of new types of ballistic fabric armor that appear on the market. For example, one such fabric is Zylon, produced by the Toyobo Corporation (Toyobo [26]), which constructed from woven PBO fibers. Zylon has recently been applied by SRI to ballistic shielding of aircraft (Shockey et al. [22], Simons et al. [23]).

In this paper a simulation technique is developed to estimate the number of ballistic fabric sheets needed to stop an incoming projectile. The technique is designed so that it can be easily implemented by a wide audience of researchers in the field, without resorting to more involved finite element formulations, by taking advantage of the intrinsic features of fabric structures. The outline of this paper is as follows. In section two, the deformation of the fabric, which is finite, nonlinearly inelastic due to progressive micro-filament rupture and dynamically coupled to the projectile, is addressed. The equations of dynamic equilibrium are also given. In section three, a recursive, temporally adaptive scheme is developed to solve the system. Theoretical issues pertaining to convergence of the algorithm are investigated. Finally, 3-D numerical examples are then given to illustrate the approach in determining the number of sheets needed to stop a projectile. Extensions to the model are then discussed.

2 A model for fiber response

Since the axial strains in the fibers comprising the fabric net are expected to be in the range of 2%–10% before rupturing, we consider a Kirchhoff-St. Venant material. In the absence of any damage, the stored energy function for such a material is $W(\mathbf{E}) = \frac{1}{2}\mathbf{E}:\mathbb{E}^Y:\mathbf{E}$, where $\mathbb{E}^Y$ is the elasticity tensor, $\mathbf{E} \stackrel{\text{def}}{=} \frac{1}{2}(\mathbf{C} - \mathbf{1})$ is the Green–Lagrange strain, $\mathbf{C} \stackrel{\text{def}}{=} \mathbf{F}^T \cdot \mathbf{F}$ is the right Cauchy–Green strain, $\mathbf{F} = \nabla_X \mathbf{x}$ is the deformation gradient and where X are referential and $\mathbf{x}$ are current coordinates respectively. Since the second Piola–Kirchhoff stress can be expressed as $\mathbf{S} = \partial W/\partial \mathbf{E}$, we may write $\mathbf{S} = \mathbb{E}^Y:\mathbf{E}$. After $\mathbf{S}$ has been computed one may write $\boldsymbol{\sigma} = \frac{1}{J}\mathbf{F}\cdot\mathbf{S}\cdot\mathbf{F}^T$, $\boldsymbol{\sigma}$ being the Cauchy stress, where J is the Jacobian of $\mathbf{F}$, $J = \det \mathbf{F}$.

Due to the thinness of the fibers, we assume a plane uniaxial-stress type condition. For the analysis of a single fiber, we align the coordinate system with the undeformed axial (x_1) state, where C_{11} is the component of $\mathbf{C}$ along the length of the fiber (Fig. 3). Due to the assumption regarding the stress state, $S_{22} = S_{33} = 0$. Because the material

Received 28 February 2002 / Accepted 2 April 2002

T. I. Zohdi
Department of Mechanical Engineering,
6195 Etcheverry Hall, University of California,
Berkeley, CA, 94720-1740, USA
e-mail: zohdi@newton.berkeley.edu

The author wishes to thank Dr. Don Shockey and Dr. Jeff Simons of SRI and Prof. David Steigmann and Prof. Werner Goldsmith of UC Berkeley for their constructive comments during the course of this research. The author also expresses his gratitude for support from FAA grant number 01-C-AW-WISU.

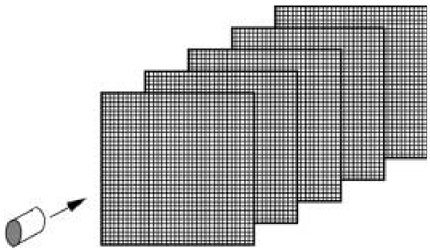

Fig. 1. A projectile encountering a multilayered fabric shielding

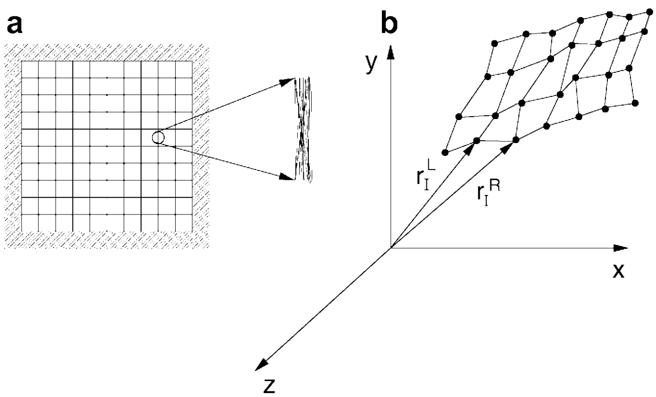

Fig. 2. **a** An idealized fabric net. **b** A possible configuration of a portion of the fabric

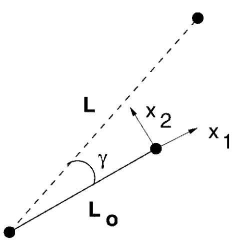

Fig. 3. A geometrical description of the deformation of an individual fiber using a locally aligned coordinate system

is assumed to be isotropic, this implies that the Cauchy stress, written in terms of a coordinate system where one axis is aligned with the deformed axial direction of the fiber, also has only one nonzero component. By setting $S_{22} = S_{33} = 0$, one obtains relations for $C_{22} = C_{33}$ in terms of C_{11}. Assuming that the material is isotropic we have

$$\begin{aligned} E_{11} &= \frac{S_{11}}{E^Y} - \nu\left(\frac{S_{22}+S_{33}}{E^Y}\right), \\ E_{22} &= \frac{S_{22}}{E^Y} - \nu\left(\frac{S_{11}+S_{33}}{E^Y}\right), \qquad (1) \\ E_{33} &= \frac{S_{33}}{E^Y} - \nu\left(\frac{S_{11}+S_{22}}{E^Y}\right) . \end{aligned}$$

Enforcing $S_{22} = S_{33} = 0$, one obtains $S_{11} = E^Y E_{11}$ and $E_{22} = E_{33} = -\nu E_{11}$. Consequently

$$[\mathbf{C}] \stackrel{\text{def}}{=} \begin{bmatrix} C_{11} & 0 & 0 \\ 0 & C_{22} & 0 \\ 0 & 0 & C_{33} \end{bmatrix} , \qquad (2)$$

where $C_{22} = -\nu(C_{11} - 1) + 1 = C_{33}$, and thus

$$J = \sqrt{C_{11}C_{22}C_{33}} = \sqrt{C_{11}(-\nu(C_{11}-1)+1)^2} . \qquad (3)$$

We may decompose the deformation gradient into a rotation and stretch, $\mathbf{F} = \mathbf{R} \cdot \mathbf{U}$. Explicitly, for an individual fiber we have $U_{11} = U_I = L_I/L_o$, $U_{22} = \sqrt{C_{22}}$, $U_{33} = \sqrt{C_{33}}$, where L_I is the deformed length of the Ith fiber, and L_o is its original length. Explicitly, the axial stretch of the Ith fiber is $U_I = L_I/L_o$. Explicitly we may write for the Cauchy stress

$$\begin{aligned} \begin{bmatrix} \sigma_{11} & \sigma_{12} & \sigma_{13} \\ \sigma_{21} & \sigma_{22} & \sigma_{23} \\ \sigma_{31} & \sigma_{32} & \sigma_{33} \end{bmatrix} &= \frac{1}{J} \begin{bmatrix} R_{11}(\gamma) & R_{12}(\gamma) & R_{13}(\gamma) \\ R_{21}(\gamma) & R_{22}(\gamma) & R_{23}(\gamma) \\ R_{31}(\gamma) & R_{32}(\gamma) & R_{33}(\gamma) \end{bmatrix} \\ &\times \begin{bmatrix} U_{11} & 0 & 0 \\ 0 & U_{22} & 0 \\ 0 & 0 & U_{33} \end{bmatrix} \\ &\times \begin{bmatrix} S_{11} & 0 & 0 \\ 0 & 0 & 0 \\ 0 & 0 & 0 \end{bmatrix} \begin{bmatrix} U_{11} & 0 & 0 \\ 0 & U_{22} & 0 \\ 0 & 0 & U_{33} \end{bmatrix} \\ &\times \begin{bmatrix} R_{11}(\gamma) & R_{12}(\gamma) & R_{13}(\gamma) \\ R_{21}(\gamma) & R_{22}(\gamma) & R_{23}(\gamma) \\ R_{31}(\gamma) & R_{32}(\gamma) & R_{33}(\gamma) \end{bmatrix}^{\mathrm{T}} \end{aligned} \qquad (4)$$

For the axial stress needed to compute fiber rupture one can simply re-write the stress tensor with respect to axes that are aligned with the deformed configuration, $\hat{\boldsymbol{\sigma}} = \mathbf{R}(-\gamma) \cdot \boldsymbol{\sigma} \cdot \mathbf{R}^{\mathrm{T}}(-\gamma)$. All components of $\hat{\boldsymbol{\sigma}}$ are zero except for the axial component, which is simply $\sigma^a = (1/J)U_{11}^2 S_{11}$.

2.1
Relaxed theory for compression

Our primary interest is to treat problems where the compressive strength of the fibers contributes negligibly to the response of the fabric. Clearly, compression of fibers will lead to buckling, and hence to wrinkling of the fabric when it is considered as a continuum. It is rather obvious that a theory where no flexure resistance (bending) and no compressive stresses are allowed cannot adequately describe wrinkling. The use of theories which take bending and compression into account involve a much higher degree of computational effort. Since the usual quantity of interest for fabrics used in structural applications is the global force-deflection (tensile) response, which is relatively insensitive to small local compressive responses, analyses based on so-called relaxed theories of perfectly flexible solids are frequently used. Essentially, such theories consist of enforcing a zero stress state for any compressive strains. Pipkin [19] appears the first to have shown that such a model is compatible with the conventional theory of elastic surfaces by considering a minimizing sequence for an associated variational problem, and that such sequences have a structure similar to observed wrinkling in thin elastic sheets. Such approaches, in one way or another, have been adopted by numerous researchers for the elastostatic analysis of structural fabric. For example, see Buchholtz et al. [4], Pangiotopoulos [17], Bufler and Nguyen-Tuong [5] and Cannarozzi [6] and [7]. In a series of works by Steigmann and coworkers: Haseganu and Steigmann [8–10] and Atai and Steigmann [2–3], a variety of theoretical results and elastostatic solution techniques based on pseudo-dynamic relaxation methods were developed. A crucial theoretical result proven by Steigmann and coworkers is that a necessary condition for the existence of energy minimizers in elastostatics is that the fibers carry no loading in compression. In the present work, we adopt this condition in the dynamic case as well, i.e. if $U_I \leq 1$, we set $\sigma^a = 0$.

2.2 Progressive damage in the fabric

The rupture of most fibers used as shielding is not sudden, but rather gradual as shown in Fig. 4. This is attributed to inhomogeneous rupture of microscale filaments which comprise a single fiber (Fig. 2), as well as internal microscale friction, which impedes micro-filament pullout between the individual micro-filaments. On the continuum scale we represent this progressive degradation in each fiber comprising the fabric net by a damage parameter

$$E_I^Y = \alpha_I E_o^Y \quad , \tag{5}$$

where for each fiber $I = 1, \ldots N$, the damage parameter is governed by the following over-stress evolution equation

$$\dot{\alpha}_I = \zeta\left(\frac{\sigma_I^a}{\sigma_{\text{crit}}^a} - 1\right)\alpha_I \quad (0 < \alpha_I \leq 1) \quad , \tag{6}$$

where if $\sigma_I^a < \sigma_{\text{crit}}$ then $\zeta = 0$ and where if $\sigma_I^a \geq \sigma_{\text{crit}}$ then $\zeta = \zeta^*$.

Remark. A microscale analysis of inhomogeneous micro-filament rupture within Zylon fibers, including thermal effects, was carried out in Zohdi and Steigmann [28] to motivate the relation in Eq. 6.

2.3 Dynamic equilibrium of the fabric net

We consider a mass lumping technique whereby at each node an equation for dynamic equilibrium is computed:

$$m\ddot{\mathbf{u}}_i = \sum_{I=1}^{4} \mathbf{f}_I + \mathbf{P}_i \quad , \tag{7}$$

where the four forces ($\mathbf{f}_I$) are the axial contributions of the four fibers intersecting at node i (Fig. 5), m is the mass of a single lumped mass node, i.e. the total fabric mass divided by the total number of nodes, and where $\mathbf{P}_i$ is the contribution from the projectile, if the node is in contact with the projectile. The cross-sectional area is given by

$$J_I A_o L_o = A_I L_I \Rightarrow A_I = \frac{J_I A_o L_o}{L_I} \quad , \tag{8}$$

and thus the forces in the current configuration can be computed by

$$\mathbf{f}_I = \sigma_I^a A_I \mathbf{a}_I = \alpha_I \frac{E_o^Y}{2} A_o (U_I^3 - U_I)\mathbf{a}_I \quad , \tag{9}$$

where the axial directions are given by

$$\mathbf{a}_I = \frac{\mathbf{r}_I^R - \mathbf{r}_I^L}{||\mathbf{r}_I^R - \mathbf{r}_I^L||} \quad . \tag{10}$$

3 A recursive solution procedure

Consider the general equation:

$$A(\mathbf{u}) = g(\mathbf{u}) \quad . \tag{11}$$

It is advantageous to write this in the form

$$\Pi(\mathbf{u}) = G(\mathbf{u}) - \mathbf{u} + \mathbf{d} = \mathbf{0} \quad . \tag{12}$$

A straightforward fixed point iterative scheme is

$$G(\mathbf{u}^{k-1}) + \mathbf{d} = \mathbf{u}^k \tag{13}$$

The convergence of such a scheme is dependent on the characteristics of G. Namely, a sufficient condition for convergence is that G is a contraction mapping for all $\mathbf{u}^k$, $k = 1, 2, 3 \ldots$. Convergence of the iteration can be studied by defining the error vector $\mathbf{e}^k = \mathbf{u}^k - \mathbf{u}$. A necessary condition for convergence is iterative self consistency, i.e. the exact solution must be represented by the scheme $G(\mathbf{u}) + \mathbf{d} = \mathbf{u}$. Using this condition, a sufficient condition for convergence is the existence of a contraction mapping

$$\begin{aligned} ||\mathbf{e}^k|| = ||\mathbf{u}^k - \mathbf{u}|| &= ||G(\mathbf{u}^{k-1}) - G(\mathbf{u})|| \\ &\leq \eta ||\mathbf{u}^{k-1} - \mathbf{u}|| \quad , \end{aligned} \tag{14}$$

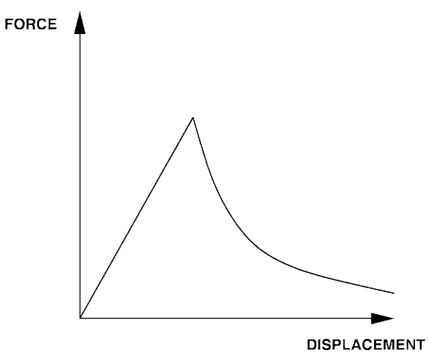

Fig. 4. A typical tensile response for fiber comprised of a group of micro-filaments

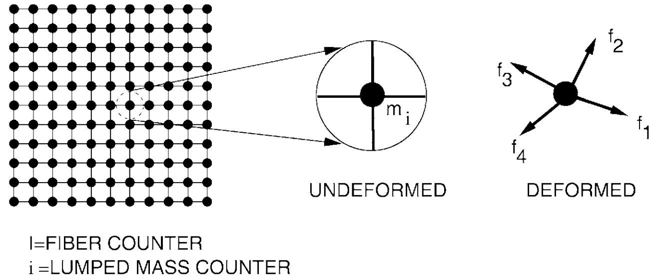

Fig. 5. A fabric comprised of lumped masses

where, if $\eta < 1$ for each iteration k, then $\mathbf{e}^k \to \mathbf{0}$ for any arbitrary starting solution $\mathbf{u}^{k=0}$ as $k \to \infty$. If G is differentiable, we may write

$$G(\mathbf{u}) = G(\mathbf{u}^{k-1}) + \nabla_{\mathbf{u}} G(\mathbf{u})|_{\mathbf{u}^{k-1}}(\mathbf{u}^{k-1} - \mathbf{u}) + \mathcal{O}(||\Delta\mathbf{u}||^2) \quad , \tag{15}$$

and thus, provided that the functional behavior is locally convex (Perron [18], Ostrowski [15, 16], Ortega and Rockoff [14] and Kitchen [12]) in the neighborhood of the solution,

$$\begin{aligned}
&||G(\mathbf{u}) - G(\mathbf{u}^{k-1})|| \\
&\quad = ||\nabla_{\mathbf{u}} G(\mathbf{u})|_{\mathbf{u}^{k-1}}(\mathbf{u}^{k-1} - \mathbf{u}) + \mathcal{O}(||\Delta\mathbf{u}||^2)|| \\
&\quad \leq ||\nabla_{\mathbf{u}} G(\mathbf{u})|_{\mathbf{u}^{k-1}}(\mathbf{u}^{k-1} - \mathbf{u})|| \text{ (local convexity)} \\
&\quad \leq \underbrace{||\nabla_{\mathbf{u}} G(\mathbf{u})|_{\mathbf{u}^{k-1}}||}_{\eta^{k-1}} ||\mathbf{u}^{k-1} - \mathbf{u}|| \quad .
\end{aligned} \tag{16}$$

Therefore, unconditional convergence is attained if for $\mathbf{u}^k$, $k = 1, 2, 3 \ldots$, $\eta^k < 1$. General overviews of fixed-point algorithms can be found in Ames [1].

Remark. A Newton-type solution scheme, which can be considered as a higher order fixed-point iteration, can be developed by writing $\Pi(\mathbf{u}^k) = \Pi(\mathbf{u}^{k-1}) + \frac{\partial \Pi}{\partial \mathbf{u}}|_{\mathbf{u}^{k-1}}$ $(\mathbf{u}^k - \mathbf{u}^{k-1}) + \mathcal{O}(||\Delta\mathbf{u}||^2) \approx 0$, thus leading to the following sufficient convergence criteria

$$\left| \left(\Pi(\mathbf{u}) \left(\frac{\partial \Pi}{\partial \mathbf{u}} \right)^{-2} \frac{\partial^2 \Pi}{\partial \mathbf{u}^2} \right) \Big|_{\mathbf{u}^{k-1}} \right| < 1 \quad . \tag{17}$$

Newton's method usually converges at a faster rate than a direct fixed point iteration, quadratic as opposed to superlinear, however its convergence criteria is less robust than the presented fixed-point algorithm, due to its dependence on the gradients of the solution. We now tailor the presented fixed-point approach to the problem at hand.

3.1 A recursive staggering scheme

Consider the following iterative scheme for all nodes not in direct contact with the projectile

$$m\ddot{\mathbf{u}}_i^k = \sum_{I=1}^{4} \mathbf{f}_I^{k-1} \quad , \tag{18}$$

where I denotes local nodes and where $k = 1, 2, 3 \ldots$ is an iteration counter. The case of nodes in direct contact with the projectile will be treated in the next section. Using a backward Euler approximation we have

$$\begin{aligned}
\ddot{\mathbf{u}}_i^k(t + \delta t) &\approx \frac{\mathbf{v}_i^k(t + \delta t) - \mathbf{v}_i(t)}{\delta t} \\
&\approx \frac{\mathbf{u}_i^k(t + \delta t) - \mathbf{u}_i(t)}{(\delta t)^2} - \frac{\mathbf{v}_i(t)}{\delta t} \quad ,
\end{aligned} \tag{19}$$

leading to

$$\mathbf{u}_i^k(t + \delta t) = \mathbf{u}_i(t) + \mathbf{v}_i(t)\delta t + \frac{(\delta t)^2}{m} \sum_{I=1}^{4} \mathbf{f}_I^{k-1} \quad . \tag{20}$$

For all nodes, at a given time step, the $\mathbf{u}^k$ are computed until

$$||\mathbf{u}_i^k(t + \delta t) - \mathbf{u}_i^{k-1}(t + \delta t)|| \leq TOL \quad . \tag{21}$$

Comparing Eq. (21) to Eq. (12), we see that

$$\begin{aligned}
G(\mathbf{u}_i^{k-1}) &\stackrel{\text{def}}{=} \frac{(\delta t)^2}{m} \sum_{I=1}^{4} \mathbf{f}_I^{k-1} \\
&= \frac{E_o^Y A_o (\delta t)^2}{2m} \sum_{I=1}^{4} \alpha_I^{k-1}((U_I^{k-1})^3 - U_I^{k-1})\mathbf{a}_I^{k-1} \quad .
\end{aligned} \tag{22}$$

Therefore the spectral radius of G grows with $(E_o^Y A_o (\delta t)^2)/(2m)$.

3.2 Substaggered projectile/fabric interaction

In order to simplify the problem somewhat, we assume that the projectile has only one velocity component, namely orthogonal to the fabric (denoted as the z-direction). Furthermore, the projectile is assumed to be rigid. Initially, the velocity can be computed from a balance of momentum in the z-direction

$$m_p v^o = m_p v_p + m_f^C v_f \Rightarrow v_{pz} = \frac{m_p}{m_p + m_f^C} v^o \quad , \tag{23}$$

where all external forces are zero due to the fact that initially, the fabric is unstretched. Here v^o is the incoming velocity of the projectile and m_f^C represents the mass of the fabric contact area. We restrict all nodes that are underneath the projectile to have the same z-component of velocity as the projectile, however, they may slide, in a frictionless manner, in any other direction. As time progresses, when the projectile and fabric are in contact, we have a work-energy

$$\begin{aligned}
&\frac{1}{2} m_p \mathbf{v}_p(t) \cdot \mathbf{v}_p(t) + \sum_{i=1}^{N} \frac{1}{2} m \mathbf{v}_i(t) \cdot \mathbf{v}_i(t) - \sum_{I=1}^{F} A_o L_o \\
&\quad \times \int_{E_{I11}(t)}^{E_{I11}(t+\delta t)} \alpha_I(t + \delta t) E_o^Y E_{I11}(t + \delta t) \mathrm{d}E_{I11} \\
&= \frac{1}{2} m_p \mathbf{v}_p(t + \delta t) \cdot \mathbf{v}_p(t + \delta t) \\
&\quad + \sum_{i=1}^{F} \frac{1}{2} m \mathbf{v}_i(t + \delta t) \cdot \mathbf{v}_i(t + \delta t) \quad .
\end{aligned} \tag{24}$$

We obtain the solution of this problem with a fixed-point iteration, which will be later embedded into an overall staggering process, $\mathbf{v}_p \cdot \mathbf{v}_p = v_{pz}^2$

$$\begin{aligned}
v_{pz}^k(t + \delta t) = (v_{pz}^2(t) &- \frac{2}{m_p} \sum_{I=1}^{F} A_o L_o \\
&\times \int_{E_{I11}(t)}^{E_{I11}^{k-1}(t+\delta t)} \alpha_I^{k-1}(t + \delta t) E_o^Y E_{I11}^{k-1}(t + \delta t) \mathrm{d}E_{I11} \\
&+ \frac{m}{m_p} \sum_{i=1}^{N} \mathbf{v}_i(t) \cdot \mathbf{v}_i(t) \\
&- \frac{m}{m_p} \sum_{i=1}^{N} \mathbf{v}_i^{k-1}(t + \delta t) \cdot \mathbf{v}_i^{k-1}(t + \delta t))^{\frac{1}{2}}
\end{aligned} \tag{25}$$

Writing $v_{pz}(t+\delta t) = (u_{pz}(t+\delta t) - u_{pz}(t))/(\delta t)$ yields the following staggering scheme

$$u^k_{pz}(t+\delta t) = u_{pz}(t) + \delta t(v^2_{pz}(t) - \frac{2}{m_p}\sum_{I=1}^{F} A_o L_o \times \int_{E_{I11}(t)}^{E^{k-1}_{I11}(t+\delta t)} \alpha^{k-1}_I(t+\delta t) E^Y_o E^{k-1}_{I11}(t+\delta t)\mathrm{d}E_{I11} + \frac{m}{m_p}\sum_{i=1}^{N} \mathbf{v}_i(t)\cdot\mathbf{v}_i(t) - \frac{m}{m_p}\sum_{i=1}^{N} \mathbf{v}^{k-1}_i(t+\delta t)\cdot\mathbf{v}^{k-1}_i(t+\delta t))^{\frac{1}{2}} \ . \tag{26}$$

For all nodes in direct contact with the projectile $u_{iz} = u_{pz}$ at all times.

3.3 Overall solution procedure

For a sheet/projectile pair:

$$v_{pz} = \frac{m_p}{m_p + m^C_f} v^o$$

Within a time step:

Step I: Solve for displacements via equilibrium: if in contact zone:

$$u^k_{ix}(t+\delta t) = u_{ix}(t) + v_{ix}(t)\delta t + \frac{(\delta t)^2}{m}\sum_{i=1}^{4} f^{k-1}_{ix} \ ,$$

$$u^k_{iy}(t+\delta t) = u_{iy}(t) + v_{iy}(t)\delta t + \frac{(\delta t)^2}{m}\sum_{i=1}^{4} f^{k-1}_{iy} \ ,$$

$$u^k_{iz}(t+\delta t) = u^{k-1}_{pz}(t+\delta t) \ .$$

If not in contact zone:

$$\mathbf{u}^k_i(t+\delta t) = \mathbf{u}_i(t) + \mathbf{v}_i(t)\delta t + \frac{(\delta t)^2}{m}\sum_{i=1}^{4} \mathbf{f}^{k-1}_i \ .$$

Step II: Solve for axial Cauchy stresses:

$$\sigma^{ak}_I = \frac{1}{J^k_I}(U^k_{I11})^2 S^k_{I11} \ .$$

Step III: Compute damage evolution:

$$\dot{\alpha}^k_I = \zeta^k\left(\frac{|\sigma^{ak}_I|}{\sigma^a_{crit}} - 1\right)\alpha^k_I \ .$$

Step IV: Compute projectile position:

$$u^k_{pz}(t+\delta t) = u_{pz}(t) + \delta t(v^2_{pz}(t) - \frac{2}{m_p}\sum_{I=1}^{F} A_o L_o \times \int_{E_{I11}(t)}^{E^{k-1}_{I11}(t+\delta t)} \alpha^{k-1}_I(t+\delta t) E^Y_o E^{k-1}_{I11}(t+\delta t)\mathrm{d}E_{I11} + \frac{m}{m_p}\sum_{i=1}^{N} \mathbf{v}_i(t)\cdot\mathbf{v}_i(t) - \frac{m}{m_p}\sum_{i=1}^{N} \mathbf{v}^{k-1}_i(t+\delta t)\cdot\mathbf{v}^{k-1}_i(t+\delta t))^{\frac{1}{2}} \ .$$

Step V: Repeat until:

$$||\mathbf{u}^k_i(t+\delta t) - \mathbf{u}^{k-1}_i(t+\delta t)|| \leq TOL||\mathbf{u}^k_i(t+\delta t)|| \ .$$

Step VI: If no converge in j iterations reduce time step size:

$$\delta t = (\delta t)_o \frac{||\mathbf{u}^k_i(t+\delta t)||TOL}{||\mathbf{u}^k_i(t+\delta t) - \mathbf{u}^{k-1}_i(t+\delta t)||} \ .$$

Step VII: Go to next time step.
reset

$$\delta t = (\delta t)_o \ .$$

Step VIII: If penetration occurs go to next sheet:

$$v^o = v_{pz}(t+\delta t) \ . \tag{27}$$

Remark. A relatively simple approximation for the work integral of the fibers needed for the displacement of the projectile is to evaluate the damaged state at the midpoint of the time interval, and then to integrate the remaining terms analytically,

$$\int_{E_I 11(t)}^{E^{k-1}_{I11}(t+\delta t)} \alpha^{k-1}_I(t+\delta t) E^Y_o E^{k-1}_{I11}(t+\delta t)\mathrm{d}E_{I11} \approx \frac{\alpha^{k-1}_I(t+\delta t) + \alpha_I(t)}{2}\frac{E^Y_o(E^{k-1}_{I11}(t+\delta t))^2}{2} \ .$$

4 An example and discussion

We considered a 50 caliber, 0.0127 m (0.5 inch) in diameter, 0.037 kg cylindrical projectile initially traveling at 304 m/s. A Zylon fabric net of 35 $\times$ 35 fibers per square inch was used. The individual fibers were taken to have effective radii of 0.00025 m. The fabric was square of dimensions 0.254 $\times$ 0.254 m, thus leading to 350 $\times$ 350 fibers, and consequently 350 $\times$ 350 lumped mass nodes and $3 \times 350^2 = 367500$ degrees of freedom (unknowns). The location of the center of the projectile at initial impact was $x = 0.7 \times 0.254$ m, $y = 0.3 \times 0.254$ m and $z = 0.0$ m

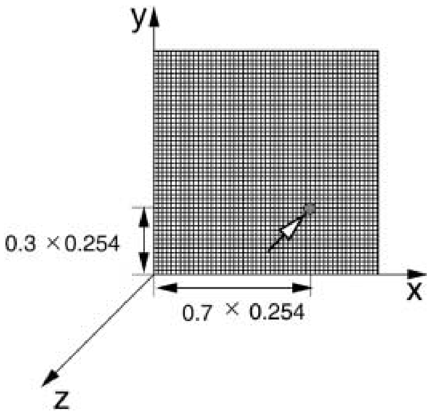

Fig. 6. Location of initial contact of the projectile

(Fig. 6). To illustrate the characteristics of the model, we used material parameters for Zylon taken from a recent technical report Toyobo [26]: $E^Y_o = 180$ GPa, $\sigma^{\text{crit}} = 6.333$ GPa and $\rho_o = 1540.0\,\text{kg/m}^3$. It was estimated from previous experimental and numerical analyses (using large-scale finite element approaches) by SRI (Shockey et al. [22] and Simons et al. [23]) that approximately 20–25 sheets would be needed to stop an incoming projectile such as the one described when hit directly in the center of the sheets ($x = 0.5 \times 0.254$ m, $y = 0.5 \times 0.254$ m and $z = 0.0$ m). The parameter fiber degradation rate that matched this estimate (22 sheets) for the model was $\zeta^* = -100$. Penetration was said to occur if the material directly underneath the projectile (in the contact zone) degraded to 25% of its original stiffness, $\langle\alpha\rangle_{\omega_p} = 0.25 = 1/(|\omega_p|)\int_{\omega_p} \alpha\, d\omega_p$, i.e. 75% damage. These parameters were then used for the off-center impact. As one can see in Fig. 7, approximately 20 sheets were needed in this case. In this and other impact scenarios, the energy absorbed per sheet is not uniform. This is controlled by the amount of energy kinetically absorbed by the sheet, as well as by the elastic strain energy absorbed by the sheet. The amount absorbed kinetically and elastically is dictated by the mode of deformation, which is a dictated by the rate of loading. Hence, the amount absorbed per sheet is not a constant function. The effects of tumbling of the projectile, as it moves through the sheets, has been neglected in the analysis. Tumbling helps the impede the projectile, since the projectile loses rotational energy through this process. Another effect is due to "dragging" of the sheets previously penetrated through the remaining sheets during the overall impact process. Also, the blunting of the projectile, due to contact with the fabric, which in many cases are coated, for example with alumina, has also been ignored in the present analysis. However, experimental and finite element analyses have been carried out by SRI to investigate such effects (Shockey et al. [22] and Simons et al. [23]). Generally, neglection of all of the mentioned effects makes the present analysis conservative, i.e. it overestimates the number of sheets needed to stop a projectile. Finally, a potentially important issue is the amount of initial slack in the fibers. Upon initial impact, if there is slack in the fibers, a large amount of the kinetic energy in the projectile will go into putting the sheet into motion, i. e., virtually pure kinetic energy transfer, with no straining of the fibers until the projectile's displacement is large enough to eliminate the slack in the individual fibers. Currently, the optimization of the effects of slack and fiber weave pattern on the performance of ballistic fabric shielding is under investigation by the author.

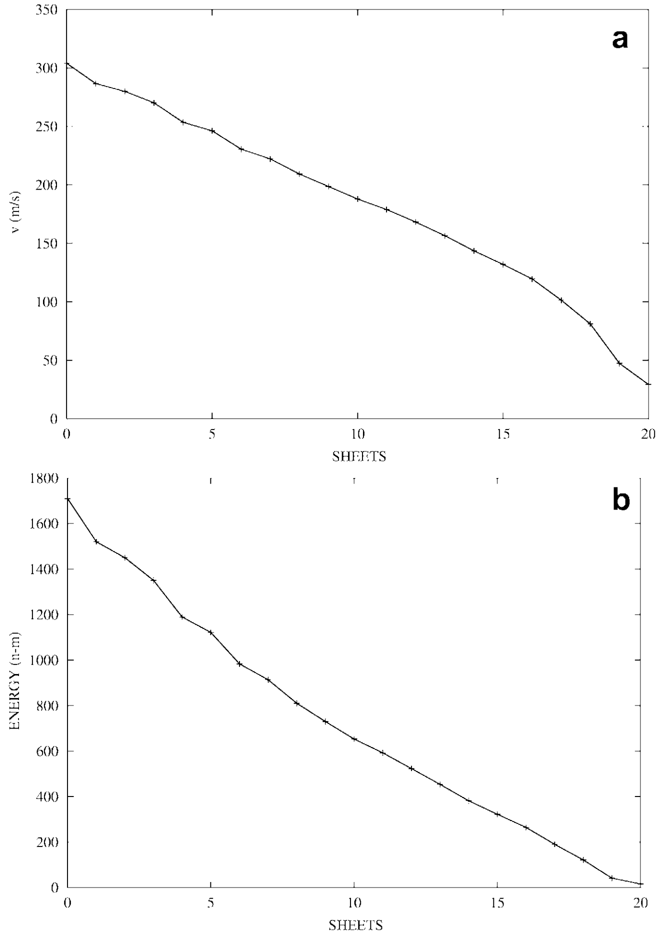

Fig. 7. a The projectile velocity as a function of the number of sheets penetrated. **b** The projectile energy as a function of the number of sheets penetrated

References

1. **Ames WF** (1977) Numerical methods for partial differential equations. 2nd Ed. Academic Press
2. **Atai AA, Steigmann DJ** (1997) On the nonlinear mechanics of discrete networks. Arch. Appl. Mech. 67: 303–319
3. **Atai AA, Steigmann DJ** (1998) Coupled deformations of elastic curves and surfaces. Int. J. Solids Struct. 35(16): 1915–1952
4. **Buchholdt HA, Davies M, Hussey MJL** (1968) The analysis of cable nets. J. Inst. Maths Applics. 4: 339–358
5. **Bufler H, Nguyen-Tuong B** (1980) On the work theorems in nonlinear network theory. Ing. Arch. 49: 275–286
6. **Cannarozzi M** (1985) Stationary and extremum variational formulations for the elastostatics of cable networks. Meccanica 20: 136–143
7. **Cannarozzi M** (1987) A minimum principle for tractions in the elastostatics of cable networks. Int. J. Solids Struct. 23: 551–568
8. **Haseganu EM, Steigmann DJ** (1994) Analysis of partly wrinkled membranes by the method of dynamic relaxation. Comput. Mech. 14: 596–614
9. **Haseganu EM, Steigmann DJ** (1994) Theoretical flexural response of a pressurized cylindrical membrane. Int. J. Solids Struct. 31: 27–50

10. **Haseganu EM, Steigmann DJ** (1996) Equilibrium analysis of finitely deformed elastic networks. Comput. Mech. 17: 359–373
11. **Johnson GR, Beissel SR, Cunniff PM** (1999) A computational model for fabrics subjected to ballistic impact. In: Proceedings of the 18th International Symposium on Ballistics, San Antonio, TX, pp. 962–969
12. **Kitchen J** (1966) Concerning the convergence of iterates to fixed points. Studia Math. 27: 247–249
13. **Kollegal MG, Sridharan S** (2000) Strength prediction of plain woven fabrics. J. Comp. Mat. 34: 240–257
14. **Ortega J, Rockoff M** (1966) Nonlinear difference equations and Gauss–Seidel type iterative methods. SIAM J. Numer. Anal. 3: 497–513
15. **Ostrowski A** (1957) Les points d' attraction et de répulsion pour l'itération dans l'espace a' n dimensions. C. R. Acad. Sci. Paris 244: 288–289
16. **Ostrowski A** (1966) Solution of equations and systems of equations. Academic Press, New York
17. **Pangiotopoulos PD** (1976) A variational inequality approach to the inelastic stress-unilateral analysis of cable structures. Comput. Struct. 6: 133–139
18. **Perron O** (1929) Über Stabilität und asymptotisches Verhalten der Lösungen eines Systems endlicher Differenzengleichungen. J. Reine Angew. Math 161: 41–64
19. **Pipkin AC** (1986) The relaxed energy density for isotropic elastic membranes. IMA J. Appl. Math. 36: 297–308
20. **Roylance D, Wang SS** (1980) Penetration mechanics of textile structures, ballistic materials and penetration mechanics. Elsevier, pp. 273–293
21. **Shim VP, Tan VBC, Tay TE** (1995) Modelling deformation and damage characteristics of woven fabric under small projectile impact. Int. J. Impact. Eng. 16: 585–605
22. **Shockey DA, Erlich DC, Simons JW** (1999) Lightweight fragment barriers for commercial aircraft. In: Proceedings of the 18th International Symposium on Ballistics, San Antonio, TX, pp. 1192–1199
23. **Simons JW, Erlich DC, Shockey DA** (2001) Finite element design model for ballistic response of woven fabrics. In: Proceedings of the 19th International Symposium on Ballistics, Interlaken, Switzerland, pp. 1415–1422
24. **Tabiei A, Jiang Y** (1999) Woven fabric composite material model with material nonlinearity for finite element simulation. Int. J. of Solids Struct. 36: 2757–2771
25. **Taylor WJ, Vinson JR** (1990) Modelling ballistic impact into flexible materials. AIAA Journal 28: 2098–2103
26. **Toyobo** (2001) PBO fiber ZYLON. Report of the Toyobo Corporation, LTD, http://www.toyobo.co.jp
27. **Walker JD** (1999) Constitutive model for fabrics with explicit static solution and ballistic limit. In: Proceedings of the 18th International Symposium on Ballistics, San Antonio, TX, pp. 1231–1238
28. **Zohdi TI, Steigmann DJ** (accepted) The toughening effect of microscopic filament misalignment on macroscopic fabric response. The Int. J. Fracture (in press)